

# Developing digital cartography in rural planning applications

Fernando J. Aguilar\*, Fernando Carvajal, Manuel A. Aguilar, Francisco Agüera

*Department of Agricultural Engineering, Almería University, La Cañada de San Urbano, 04120 Almería, Spain*

Received 16 March 2006; received in revised form 21 December 2006; accepted 22 December 2006

## Abstract

The main objective of the present study is to develop an efficient methodology at a reasonable cost, that will allow the use of the latest technological developments in the areas of image analysis and geographical information systems (GIS) for the generation, compilation, operation and updating of digital cartography on a large scale in rural environments. The various possibilities offered by the current analytic cartography allow the utilization of this spatially geo-referenced database to obtain quantitative and qualitative information of great interest for the study of planning, land organization and sustainable rural development.

The methodological proposal to achieve this objective consists of three well differentiated phases: the generation of digital cartography from 1:5000 scale colour aerial photographs, the compilation of cartographic information obtained in an open architecture GIS, and, finally, the periodical updating of the GIS cartographic database by means of digital treatment and geometrical modelling of high resolution satellite imagery.

The methodology described above is being developed and applied in a specially interesting rural milieu, like “El Campo de Níjar”, located in the province of Almería (Spain) on the border with the nature reserve “Parque Natural de Cabo de Gata”.

© 2007 Elsevier B.V. All rights reserved.

**Keywords:** GIS; Rural planning and development; Digital aerial photogrammetry; Cartography updating; High resolution satellite

## 1. Introduction

There are numerous definitions of geographical information systems (GIS). A widely accepted definition is that given by Burrough and McDonnell (1998), which defines a GIS as a powerful set of tools for collecting, storing, retrieving, transforming and displaying spatial data from the real world for a particular set of purposes.

Nowadays, the applications of GIS are innumerable. The various possibilities that analytical cartography offers allow the use of geo-referenced data from these systems and the obtaining of quantitative and qualitative information of great interest. GIS is also widely utilised in studies of natural resources management, transport planning, evaluation of land capacity to house a certain activity and assessment of its impact on the environment, risk assessment of potential flooding in urban areas, military applications, analysis of potential erosion in a basin and tracking of desertification processes, etc. (Franklin, 2000; Davis and Wang, 2001; Wei and Leberg, 2002).

The generation, maintenance and exploitation of GIS require a spatial database or digital cartography, in both raster and vector formats, on which the different layers of alphanumeric information can be positioned (Burrough and McDonnell, 1998). Thus, the Autonomous Community of Andalusia (Southern Spain) possesses a series of spatial reference bases on different scales. With regard to regional ground reconnaissance, there is the LANDSAT TM mosaic

\* Corresponding author. Tel.: +34 950015339; fax: +34 950015491.  
E-mail address: [faguilar@ual.es](mailto:faguilar@ual.es) (F.J. Aguilar).

image with a resolution of 30 m/pixel. With regard to semi-detail, there is the mosaic generated from SPOT images with a resolution of 10 m/pixel, whilst on the detail level we can count on the IRS (Indian remote sensing) satellite images which offer a resolution of 5 m/pixel. At the same time, 1 m/pixel colour orthoimages (eight bits per RGB channel) have been produced by the Andalusia government from a 1:60,000 colour aerial photography, encompassing the totality of the Andalusian community. More recently, orthoimages with a geometric resolution of 0.5 m (1:5000 equivalent scale) and radiometric resolution of eight bits from 1:20,000 panchromatic aerial photographs have just appeared on the market.

However, it would not be possible for some of the potential applications of GIS on a local scale to measure up with the resolution of spatial information available on a regional level. To this we must add the necessity to update cartography, since it rapidly becomes obsolete when used to characterise such dynamic systems as the intensive crop production typical of a province like Almería (Southeast Andalusia).

The same could be said with regard to the characterisation and evaluation of erosion phenomena or studies related to desertification processes. We must note that conventional updating cycles in cartography take place at intervals of between 5 or 10 years, due to their high economic cost, which is totally insufficient for the adequate maintenance of a local scale GIS seeking to be efficient.

On the other hand, any attempt aimed at planning and organising the territory requires the physical support of a digital elevation model (DEM) (Aguilar et al., 2005a). On a local scale, the quality and accuracy of this DEM must be very high, providing GIS with a vertical dimension which allows them, for example, to capture 3D information from an area in a 2D environment. Because GIS and DEM complement each other it is possible to successfully approach studies of great interest for the rural environment, such as modelling the recharge on a watershed (Rogowski, 1996) or modelling the water quality and its contamination by agricultural fertilisers (Ararkere and Molnau, 1994; Pandey et al., 2005).

The DEMs are also necessary to generate orthoimages. Orthoimages are raster maps which store, in a geo-referenced system, all the graphic information that can be extracted from a particular zone. This type of digital cartography is generated from aerial photographs or satellite images, correcting geometrical deformations caused by scale variations, relief displacements, geometry of the sensor, earth curvature, etc. (Mikhail et al., 2001). Orthoimages, together with DEMs, are becoming the main cover of GIS, providing a rapid and cost effective methodology for updating spatial information, which allows for briefer conventional cycles for cartographic updating, highly relevant in GIS orientated to local scales.

The main objective of this study is the development of an efficient and cost-effective methodology which will allow the use of the latest technology in the area of digital imagery analysis and GIS for the production, compilation, exploitation and updating of digital cartography on a large scale in rural environments.

The methodology described subsequently is being developed in and applied to a rural environment of particular interest such as “El Campo de Níjar”, located at the Mediterranean coast of Spain (Almería, South-Eastern Spain), just on the border with the nature reserve “Parque Natural de Cabo de Gata” (Fig. 1). It is a rural and low population density zone characterized by a Mediterranean semiarid climate with an averaged annual rainfall around 250 mm. A few decades ago there only was subsistence agriculture in this area, but the recent development of a flourishing intensive agriculture under plastic sheeting, and the consequent arrival of high technology production methods, is leading up to a socioeconomic development of such magnitude that it is compromising its own sustainability. In fact, this is at present the most dynamic zone in Almería in terms of greenhouse surface growth, with approximately 6000 ha of greenhouses concentrated on a district of around 20,000 ha on the whole.

## 2. Methodological proposal

To achieve the objective proposed above, we intend to develop three well-differentiated phases:

- (1) The generation of good quality basic cartography on a large scale.
- (2) The integration of cartographic information obtained in a GIS for its subsequent exploitation.
- (3) The periodical updating of the GIS cartographic database.

### 2.1. Basic cartography development

The framework of basic cartography consists of three complementary cores: digital elevation models, orthoimages and vectorial cartography.



Fig. 1. Location of the working area.

### 2.1.1. Photogrammetric flight

The original material for the generation of basic cartography was a colour photogrammetric flight on a scale of 1:5000, approximately, with a 60% and a 25% forward and side overlap, respectively, and east–west direction of the strips. The area encompassed by the flight corresponds to the Níjar district, comprising a total of 18,354 ha, distributed in 29 strips and 670 photographs.

The metric camera used was a RMK TOP 15 (Intergraph Inc., Huntsville, Ala.) with a wide-angle lens, focal length of 153.33 mm, forward movement compensation system, angular motion control system, and automatic control for exposure by microprocessor.

The application of the technique called kinematic global positioning system (GPS) airborne control permitted us to determine the position of the projection centre of the camera ( $X_0$ ,  $Y_0$ ,  $Z_0$ ) at the moment of exposure for each photogram. These data were only utilised for initial approximations of the projection centres as additional observations in the aerotriangulation bundle adjustment (Wolf and Dewitt, 2000), i.e. they were not used to compute each strip drift parameter and so to compensate for GPS signal errors. This procedure allowed us to significantly strengthen the

definition of the absolute orientation parameters in each photogram and to facilitate the automatic point measurement and the bundle adjustment.

To carry out the kinematic GPS airborne control, we used a permanent GPS station (reference station) located in Seville (Spain). The receiver was a bifrequency TRIMBLE 4000SI model (Trimble Navigation Ltd., Sunnyvale, Cal.), with a TR GEOD L1/L2 GPS antenna. The airborne GPS receiver used was the NovAtel Millennium GPSCard.2 bifrequency model (NovAtel Inc., Calgary, Canada) with a NovAtel L1/L2 GPS antenna model 512, mounted on the vertical of the projection centre of the camera. The maximum distance between the airborne receiver and the reference basis was always less than 325 km, whilst the register for observations or epochs in both receivers was always equal to 1 s.

#### 2.1.2. Photogram scanning

The negatives were scanned with a Vexcel UltraScan5000 Precision photogrammetric scanner (Vexcel Inc., Boulder, Col.) using a geometric resolution of 20  $\mu\text{m}$  and a radiometric resolution of 24 bits (eight bits per RGB channel).

#### 2.1.3. Ground control for aerial photogrammetry

The ground control consisted of a survey campaign needed to determine the planimetric and altimetric coordinates of the photogrammetric control points and check points. These check points were taken to estimate the accuracy of the work. The coordinates of the control and check points were referred to the ED-50 European Datum (Hayford international ellipsoid), using the UTM projection. The vertical datum will take the geode as reference surface, adopting as null orthometric height point the medium level in the calm seas of Alicante (Spain). In the first place, a network of bases was constructed, supported by the Spanish geodetic network (lower order network) with the idea of increasing its density by triangulation, which allows the verification, compensation and adjustment of the network.

The bases network was supported by three survey points belonging to the national geodetic network obtained using spatial techniques, such as Castillico, Morron and Cuesta Colorada, the coordinates of which are known in the reference system called world geodetic system 1984 (WGS-84).

The observations of these bases were done in static mode by four Trimble Navigation GPS receivers, of which two were 4700 models and two 4800 models (Trimble Navigation Ltd., Sunnyvale, Cal.). The 4800 models were installed on the Castillico and Morron survey points, whereas one of the 4700 models was placed on each of the bases for a minimum observation of 10 min, obtaining the baselines that constituted two triangles for each point. In order to place each basis within an exterior compensation triangle, an auxiliary point situated close to the town of Níjar was used, with a priori undefined coordinates in the local system. The elevation mask was of 15°.

Once the static measurement data had been processed using the wave processor module of trimble geomatic office (TGO, 2002), a network was obtained, as observed in system WGS-84. Thus, a set of redundant observations of the location of the bases was acquired, which required an adjustment to and compensation process in the network. This process was carried out with the network adjustment module of trimble geomatic office (TGO, 2002).

Using this procedure, and once the good fit of the adjustment of the network in the WGS-84 system had been verified, we proceeded to convert the coordinates of the bases to the ED-50 local system by means of a 3D Helmert seven parameters transformation. In order to determine the transformation parameters we needed to know the coordinates of at least three points in both global and local systems. In our case we had WGS-84 and ED-50 coordinates with five points.

Ground control points and check points were obtained using a total GPS 4800 Trimble station working in real time kinematic mode (RTK). All the 29 RTK radiations carried out were supported on at least three bases, the coordinates of which were determined during the adjustment and compensation of the statically observed network. In this way, it was possible to orientate each figure radiated in RTK and correct it planimetrically and altimetrically. Later on, we proceeded to carry out a planimetric and altimetric compensation of the adjustment errors between the points of the coordinates known for each radiation. The correction calculations of each RTK radiation were done and the errors obtained with the software trimble geomatic office (TGO, 2002). As a final result of the methodology described above, the UTM ED-50 coordinates were obtained as well as the orthometric levels with 254 photogrammetric ground control points and 80 check points.

#### 2.1.4. Digital photogrammetry workflow

Image orientation is a prerequisite for any task involving the computation of three-dimensional coordinates such as the generation of a digital terrain model, the computation of orthoimages, and the acquisition of data for GIS.



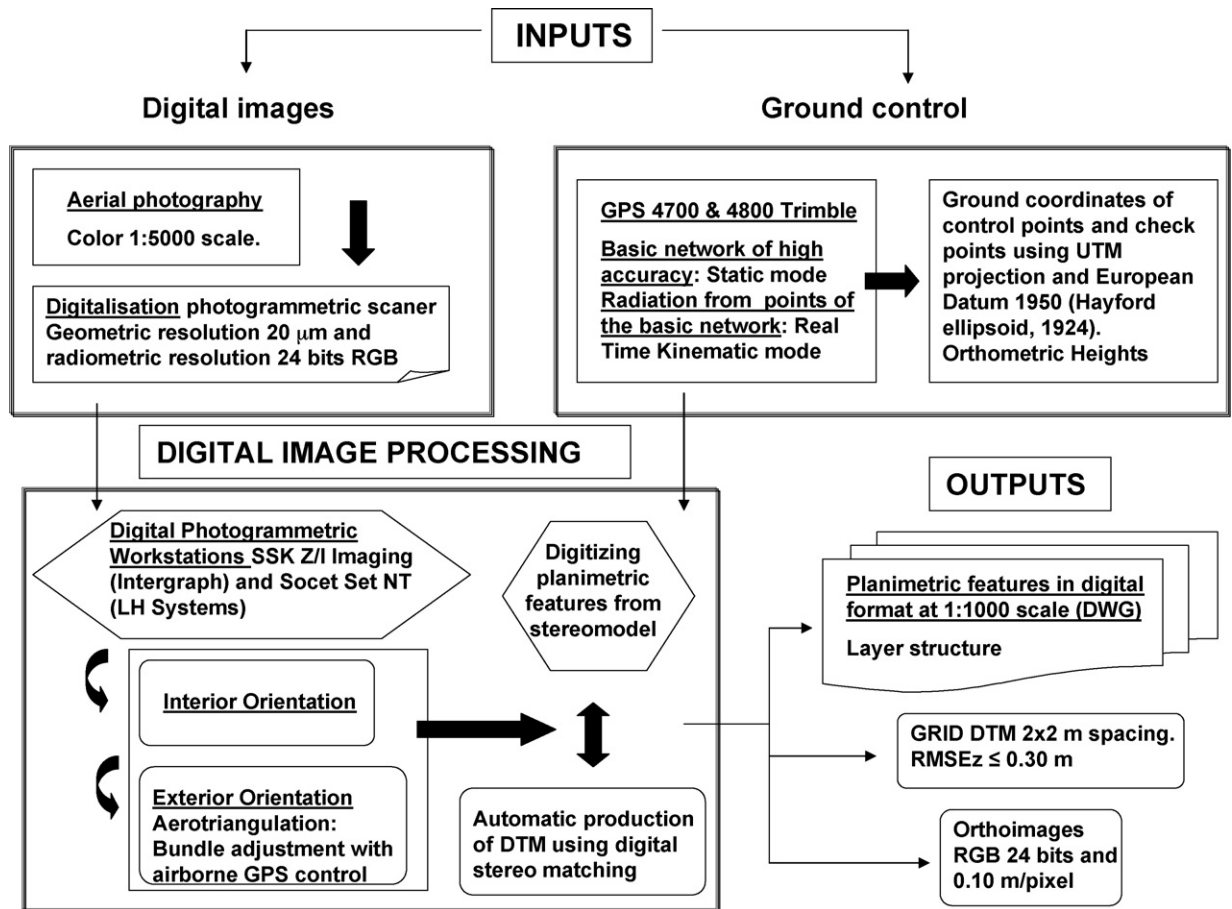


Fig. 2. Scheme flowchart of the proposal methodology to develop the basic digital cartography.

The digital processing of the information was carried out with four digital photogrammetric workstations (DPWs): two SSK Z/I Imaging (Intergraph Inc., Huntsville, Ala.) and two Socet Set NT (BAE Systems Inc., San Diego, Cal.). In Fig. 2, a flowchart diagram is shown of the methodology employed to generate this cartography.

The first step of the digital photogrammetric process is to import the digital images into the DPW, i.e. the loading of digital images and the generation in a batch mode of image pyramid levels for measurements, display and zooming. The GPS photo centre coordinates of each image is also automatically imported to provide initial values of overlaps between images (McGlone et al., 2004). At the same time, GPS ground control point data, cartographic projection and datum, and camera calibration report should be added into the project.

The second step concerns with the determination of the relationship between the pixel and the image coordinate system by means of a 2D transformation. This process is usually called “Interior Orientation”. In our case, the six parameters affine transformation was applied to relate the measurement of fiducials marks on the digital imagery with their corresponding photo coordinates. Once the fiducials on the first photo have been measured, all the fiducials on subsequent photos can be automatically measured using image correlation techniques because the approximate location of the fiducials on the image, their size, shape and brightness are known.

The last step would be the description of the transformation between the image and the object coordinate system. It is the so-called “Exterior Orientation” consisting in computing the projection centres and camera angular orientation of each photo. In modern digital photogrammetry, and for mapping projects involving more than two images, an aerial triangulation is carried out for point densification, followed by a separate exterior orientation for each model. Indeed, digital aerotriangulation is a photogrammetric technique which, from a minimal number of ground control points and through measurements in the photograms, determines the spatial coordinates of

unknown pass and tie points and the exterior orientation parameters of all photographs in the photogrammetric block.

Digital aerotriangulation are currently divided in three steps which include automatic and interactive point measurement of image coordinates (by digital matching procedures), simultaneous solution of the bundle adjustment for each photogrammetric block and, finally, blunder detection. Matching algorithm employs hierarchical methods to reduce the ambiguity problem and to extend the pull-in range. In this way, image pyramids with different resolutions are used for a coarse-to-fine strategy. In each pyramid level the following steps are performed:

- (1) Automatic initialization of the tie point areas (tie point pattern is preferably selected at the von Gruber positions where the best multi-image tie points are located).
- (2) Preliminary image matching using a combination of feature-based and least squares matching for obtaining evenly distributed tie points over the whole block.
- (3) Robust bundle block adjustment for automatic tie point selection and for the initialization of the next pyramid level.
- (4) In the last pyramid level the internal block adjustment supplies the final adjustment result. In weak block areas or bad connected strips tie points may be added by interactive point measurement in a semi-automatic mode. After manually adding points, the internal block adjustment can be started again, without repeating the matching process.

Automatic blunder detection can be driven after each run of the bundle adjustment to remove all image points with residuals over a specified threshold (e.g. over 1 pixel).

Therefore, in the exterior orientation process the ground control points obtained in the previous section have been used as well as the numerous pass and tie points resulting from the aerotriangulation process (McGlone et al., 2004). These automatically determined exterior orientation parameters are more reliable than those from the analytical solution, since blunders can be easily detected due to the high redundancy.

#### 2.1.5. Digital terrain model (DTM)

This is a DEM from which micro-relief and vegetation have been removed (buildings, infrastructures, greenhouses, etc.). DTM has been carried out by means of stereo matching techniques ranking over digital images and subsequent revision and edition by the operator (Karras et al., 1998). It is basically a process where, knowing the exterior orientation of each stereo model image, parts of an image are matched with parts of another image to reconstruct three-dimensional object information from two-dimensional projections. The stereoscopic superimposing characteristics that DPWs allow were of great help for the revision and edition tasks.

#### 2.1.6. Orthoimages

Very high resolution orthophotographs (0.10 m/pixel) and mosaics were obtained of the area under study applying the differential rectification method (Novak, 1992). For this purpose, all the orientation parameters of the images (interior and exterior) were used as well as the generated DTM.

The sampling method used in the orthoprojection process was bilinear with an automatic radiometric adjustment. In this respect, it is important to indicate that in some of the mosaics generated there are relevant radiometric differences which have been reasonably corrected using the modules IRAS-C v.8 from Z/I Imaging<sup>TM</sup> (Intergraph Inc., Huntsville, Ala.) and DODGER from Socet Set<sup>TM</sup> (BAE Systems Inc., San Diego, Cal.). The procedure followed was the approximation of histograms with similar textures by comparing their means and variances. As regards the delimitation process of the seamlines for joining the orthophotographs and constructing the final mosaic, this was done manually, as the automatic procedure produced frequent matching errors in the micro-relief elements (not contemplated in the DTM).

### 2.2. Integration of the cartographic information in a GIS

This constitutes the second phase of our study, comprising the tasks inherent to the organization and preparation of the spatial and alphanumeric information in a geo-referenced database. The chosen GIS environment was Geomedia Professional 5.1<sup>TM</sup> software, developed by Intergraph Corporation (Huntsville, Ala.). Geomedia is remarkable for its capacity to integrate data from different origins and for being user-friendly. Analysis tools such as spatial queries, attributes, areas of influence, spatial and thematic overlapping and others, solve a great number of the applications

required in rural planning. Their nature, with scaled technology and open architecture, allows the acquisition of modules to resolve specific problems or the creation of personalized applications designed by the user. In this respect, it is worth highlighting that this software allows the use of environment programming based on standard tools such as Microsoft Visual Basic®, Microsoft C++® and Delphi®.

### 2.3. Updating of the cartographic database of the GIS

In this phase a methodology is being developed that will allow us to shorten the updating of the conventional cycles in cartography on a large scale by using both panchromatic images from the QuickBird satellite (DigitalGlobe Inc., Longmont, Col.), with a geometric resolution of 0.61–0.72 m and a radiometric resolution of 11 bits/pixel, and multi-spectral images corresponding to near-infrared, red, green and blue bands, with a geometric resolution of 2.44–2.88 m and a radiometric resolution of 11 bits/pixel. Thus, planimetric and altimetric updating could be differentiated using QuickBird Basic Stereo Pair to generate DTM and single scenes (basic imagery) to update the 2D spatial database (Fig. 3).

For this purpose, QuickBird Basic Imagery was acquired on 19 December 2004, registering the following characteristics: geometric resolution of 0.62 m in panchromatic; geometric resolution of 2.49 m in visible and near-infrared spectrum; radiometric resolution of 11 bits (2048 grey levels); off nadir angle of 8°; target azimuth of 303°; cloud cover of around 6%; and finally an approximate environmental quality of 90 over a maximum value of 100.

QuickBird Basic Imagery products are radiometrically corrected and sensor corrected by the part of the vendor (DigitalGlobe Inc., 2006). Radiometric and sensor corrections do not comprise geometric correction nor mapping to a cartographic projection or ellipsoid. Atmospheric corrections are not applied either. Sometimes and for certain

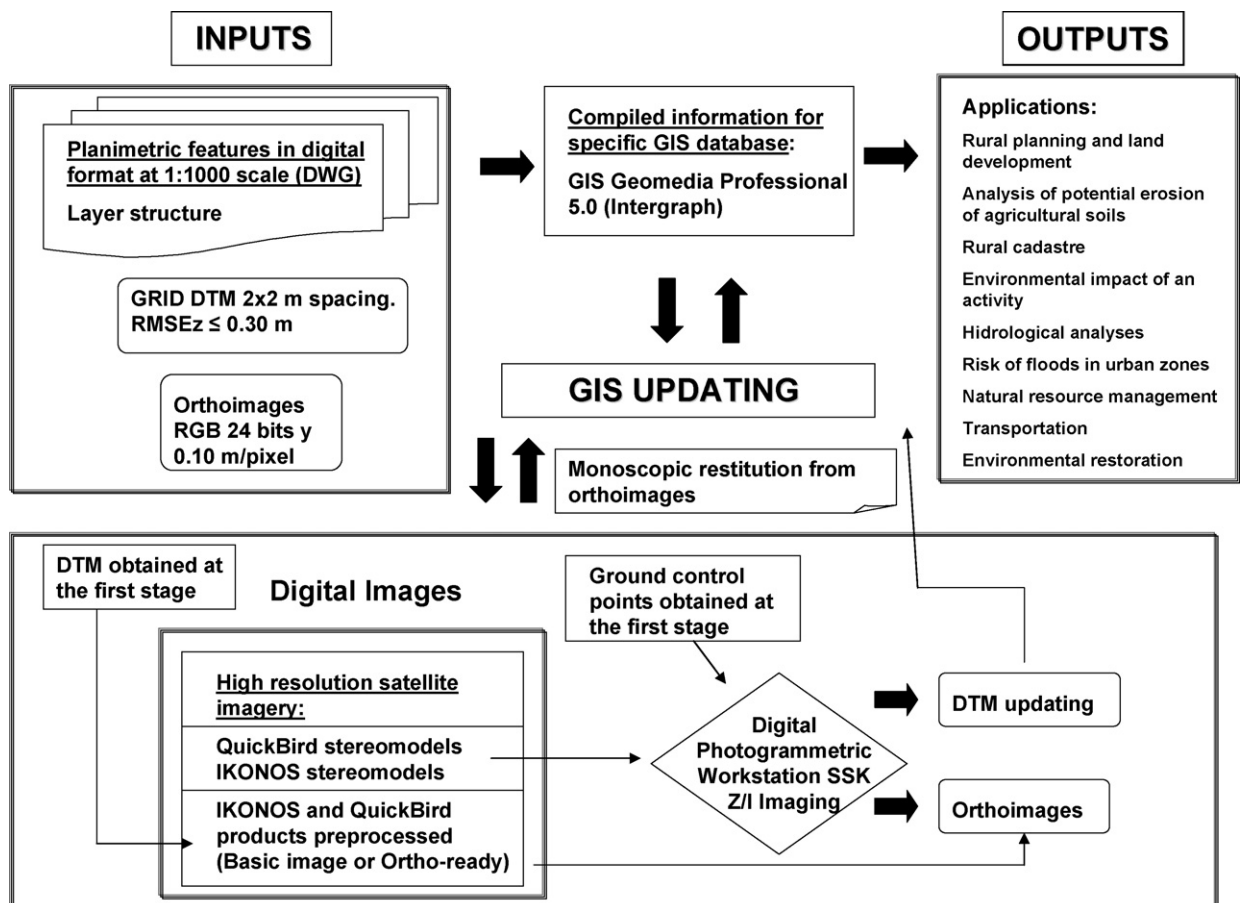


Fig. 3. Scheme flowchart of the proposal methodology for generating the GIS database and its updating.

applications from optical satellite sensors, land information is masked, since the signal recorded consists of several components with magnitudes dependant on atmospheric conditions (Richter, 1990). In this way, topographic effects strongly influence the recorded signal. The main objective of an atmospheric/topographic correction is the elimination of atmospheric and illumination effects to retrieve physical parameters of the earth's surface such as reflectance, emissivity and temperature. Processes such as path radiance, atmospheric absorption of the ground reflected radiance and scattering ground reflected radiance into the neighbourhood of the observed pixel may be considered as very common. For applications related to monitoring, change detection, climatic modelling, crops detection, and, on overall, image segmentation methods focused on the management of multispectral information, it is almost always needed to carry out some type of atmospheric correction (Wu et al., 2005). However, when the satellite imagery is utilised to extract mainly geometric information (roads, greenhouses, buildings, etc.), only a geometric correction is usually afforded. That was our case, where 3D Toutin's physical model (Toutin et al., 2002) was employed to geometrically correct and geo-reference QuickBird images from high precision ground control points measured by differential global positioning system (DGPS). Details of this procedure can be obtained from Aguilar et al. (2005b).

Once geometric correction was made, we sought to obtain almost automatically a thematic map, similar to land use/cover, in order to update our cartographic database. Therefore we had to select an imagery classification method. Most of the imagery classification methods are based on the statistical analysis of each separate pixel, having shown a good behaviour when they were used for images with a relatively large pixel size (Wang et al., 2004). But in very high resolution imagery, with a smaller pixel size, the detectable spectral variability may increase within a particular target class, making the classification even harder, especially in the case of anthropogenic structures (Kiema, 2002). To avoid this problem as far as possible, we decided to use an artificial neural network, in which we not only utilised visible and near-infrared bands, but also used a context analysis as input data. In this way, output classes were assigned to nine selected land use/cover classes such as soils with no, low and high vegetation, greenhouses with no, low, medium and high photosynthetic activity, and, finally, water and asphalted soil covers.

In the first stage of this development, we looked for an accuracy classification, since if a neural network can discriminate all interesting classes exactly, it will be able to detect changes on a cartographic database (Xiao et al., 2002).

Being similar to the human nervous system, an artificial neural network consists of a set of interconnected nodes called neurons (see Fig. 4). Its outlet depends on weighted inlet information from all inlet nodes (Tsoukalas and Uhring, 1997).

Neurons are usually clustered in functional units or levels. After different designs were attempted, the neural network chosen for this study was composed of three levels. The inlet level neurons were conformed by the four channels of the multispectral satellite image plus one more corresponding to the texture analysis result. The outlet level neurons were assigned to the nine land use/cover classes. Finally, one hidden level composed of seven operational neurons was implemented.

Texture is one of more important defining characteristics of an image. It can be estimated characterising the spatial dependency of the digital level of pixels in a neighbourhood.

One of the most frequently used texture analyses is the grey level co-occurrence matrix (e.g. Haralick et al., 1973, 1987) based on second order statistics. The grey level co-occurrence matrix is the two-dimensional matrix of joint probabilities  $P_{ij}$  between pairs of pixels, separated by a certain distance, in a given direction.

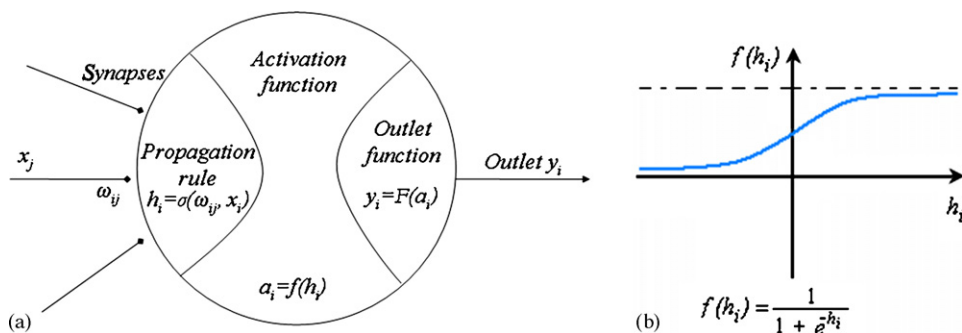


Fig. 4. Artificial neuron: (a) schema, and (b) activation function.



The statistics obtained in a first position of the mobile window are assigned to the central pixel and transferred to a texture image. Then, the window is displaced by one pixel and a new co-occurrence matrix is calculated. The window must be squared with odd number of pixels and its size should be close to the target size to be discriminated by means of the texture analysis. In this study, we chose a texture analysis based on homogeneity, calculated within a  $17 \times 17$  pixels size window, which represents a real square of about 40 m side, close to the average size of greenhouses. Due to the lack of a predominant direction in greenhouses buildings, no arrangement direction was established, considering isotropy inside the co-occurrence matrix. A near-infrared band was the inlet band because it represents well the variability related to the photosynthetic activity.

With regard to statistical analysis, homogeneity yields high values when the co-occurrence matrix shows high values in the main diagonal. This happens when the image is locally homogeneous inside a mobile window. Homogeneity is calculated according to Eq. (1):

$$\sum_{i,j=0}^{N-1} \frac{P_{ij}}{1 + (i - j)^2} \quad (1)$$

Back-propagation method (Tsoukalas and Uhring, 1997) was used to train our neural network by means of the forward and backward travelling of the information. It starts with a set of initial weights associated to the relationship between pairs of neurons (or synapses). These values change depending on the error committed in the classification, following “Generalized Delta Rule”. This process is repeated iteratively until convergence is reached in two phases.

Firstly a set ( $x_p$ ) of  $N$  inlet data is introduced in the neural network. This set is propagated forwards in the network, delivering an outlet ( $y_p$ ), which is compared with the target data ( $d_p$ ) obtained from training sites. Then, the classification error in the training process ( $e_p$ ) is computed according to a global error function (Eq. (2)):

$$e_p = \frac{1}{2} \sum_{p=1}^N \sum_{k=1}^M (d_{pk} - y_{pk})^2 \quad (2)$$

where  $k$  is the neurons outlet index in last level and  $M$  the total number of neurons in that level. Secondly, the classification error is propagated backward, modifying weight factors  $w_p$  according to Eq. (3) known as generalised delta rule (Rumelhart et al., 1995):

$$\Delta w_{ji}(t+1) = \eta \frac{\partial e_p}{\partial w_{ji}} + \alpha \Delta w_{ji}(t) \quad (3)$$

where  $\eta$  is the learning rate and  $\alpha$  is the momentum factor. The iterative process finishes when the difference between classification error in two consecutive iterations  $t$  and  $t+1$  falls below a threshold value.

It is likely that one of the land use/cover classes in our cartographic database that is subject to the greatest changes is greenhouses. Greenhouses are structures designed to protect horticultural crops against environmental agents, mainly the wind and low temperatures. Previous information about the greenhouse distribution in the study zone is scarce. Therefore, an unsupervised classification was applied to generate reference information and delineate training site boundaries. However, this was not enough because most of the target classes were related to vegetation. Because a greenhouse plastic roof is partially transparent, the digital level of a pixel belonging to a greenhouse should be influenced by photosynthetic activity.

Taking into account that chlorophyll pigments are absorbent in the red band and reflective in the near-infrared band, a vegetation index was estimated from the differences between the digital levels in those bands for each pixel. A selection of training sites was carried out thanks to the overlap of unsupervised classification and vegetation index. Thus, four greenhouse classes and three soil classes were differentiated depending on their photosynthetic activity level. Furthermore, water class and asphalted soil class were added to the process.

Unsupervised classification, vegetation index, training sites delimitation, homogeneity calculation, design and training of neural network, classification using this neural network, and accuracy estimation were carried out by means of PCI Geomatica® software (PCI, 2003).

### 3. Results and discussion

#### 3.1. Ground control for aerial photogrammetry

The triangles that constituted the network observed statically, with an external perimeter of 85 km, presented some tolerable geometrical lock errors (computed in the WGS-84 system). The geometric lock errors in the network showed the following root mean square errors:  $RMSE_{xy} = 3.84$  cm;  $RMSE_z = 5.67$  cm.

These errors are absolutely tolerable and compensable in the network adjustment. In fact, the movement of each point in the adjustment to form the compensated network was very small. Horizontal displacements lower than 2 cm were observed in the majority of cases. The average displacement in level was also acceptable and lower than 4 cm. On the other hand, the error ellipses of each point within the network are in general fairly homogenous, with deviations in planimetry which fluctuate between 6 mm from the auxiliary point to approximately 3 cm from the B-22 base. In altimetry, the deviations are of the same magnitude.

Once the principal network had been approved, we proceeded to the GPS radiation in RTK mode of the ground control points and check points. Please note that in the majority of cases the baselines have a length of about 5 km, which ensures a certain precision in the observations carried out. To be specific, the nominal error in a Trimble GPS 4800 station, working under the conditions indicated above, is of the order of 2 cm in planimetry and 2.5 cm in altimetry. In fact, the RMSEs of the planimetric and altimetric fittings of the RTK radiations in the network observed statically are lower than 5 cm.

As an additional measure to ensure the accuracy of the photogrammetric ground control in absolute terms, some survey points from the area were included in the RTK radiations, such as Cerro Gordo, Ramayo, El Hacho, Yeguas, Morales and Cabo de Gata. The absolute planimetric RMSE in these points was of 11.6 cm, whereas the vertical RMSE presented a value of 11.1 cm.

#### 3.2. Aerotriangulation

Due to the high number of photograms which compose the flight and in order to optimise the yield of the productive chain, the work was divided in three photogrammetric blocks: north, centre and south. In any case, each block shared a strip with its immediate neighbour. This procedure ensures a correct match between the different blocks.

The results that appear in Table 1 were obtained after an iterative refinement and adjustment process of each block. The internal accuracy of each block ( $\sigma_0$ ), expressed as the RMSE (image coordinates) considering the pass, tie and control points, was well below one pixel in every case (20  $\mu$ m), which verifies the good fit of the adjustment. Note that the large number of measured points per image (pass and tie points), and their good distribution in the image provided a high reliability in the adjusted camera station coordinates. In this sense, Ackermann (1996) coined the phrase “replace intelligence by redundancy”. In fact, one of the major advantages of digital photogrammetry is the potential to automate production processes efficiently, thus substantially improving the price/performance ratio for photogrammetric products.

The RMSE calculated at the ground control points was lower than 10 cm in the three components  $X$ ,  $Y$  and  $Z$  (Table 1). The maximum errors registered are also reasonable, below 18 cm in all the components. In this way, the RMSE calculated at 80 independent check points (ICPs), i.e. ground points which were not taken into account for the process of bundle adjustment, was also very low. Indeed, the aforementioned RMSE at ICPs was lower than 12 cm for the three components  $X$ ,  $Y$  and  $Z$  (Table 1). Therefore, these results are indicative of the quality of the exterior orientation parameters obtained.

Table 1

Accuracy of the aerotriangulation process measured as RMSE at ground control points (GCPs) and independent check points (ICPs)

| Photogrammetric block | Number of photograms | RMSE <sub>X</sub> (cm) |      | RMSE <sub>Y</sub> (cm) |      | RMSE <sub>Z</sub> (cm) |      | $\sigma_0$ ( $\mu$ m) |
|-----------------------|----------------------|------------------------|------|------------------------|------|------------------------|------|-----------------------|
|                       |                      | GCPs                   | ICPs | GCPs                   | ICPs | GCPs                   | ICPs |                       |
| North                 | 110                  | 6.3                    | 10   | 8.2                    | 9.5  | 6.7                    | 9.3  | 6.2                   |
| Centre                | 351                  | 8.6                    | 9.7  | 8.6                    | 11.3 | 8.3                    | 11.8 | 10.9                  |
| South                 | 258                  | 9.4                    | 11.2 | 9                      | 10.5 | 8.1                    | 11.2 | 8.3                   |

Internal accuracy of the block ( $\sigma_0$ ) measured as RMSE (image coordinates) considering the pass, tie and control points. Image pixel size = 20  $\mu$ m.

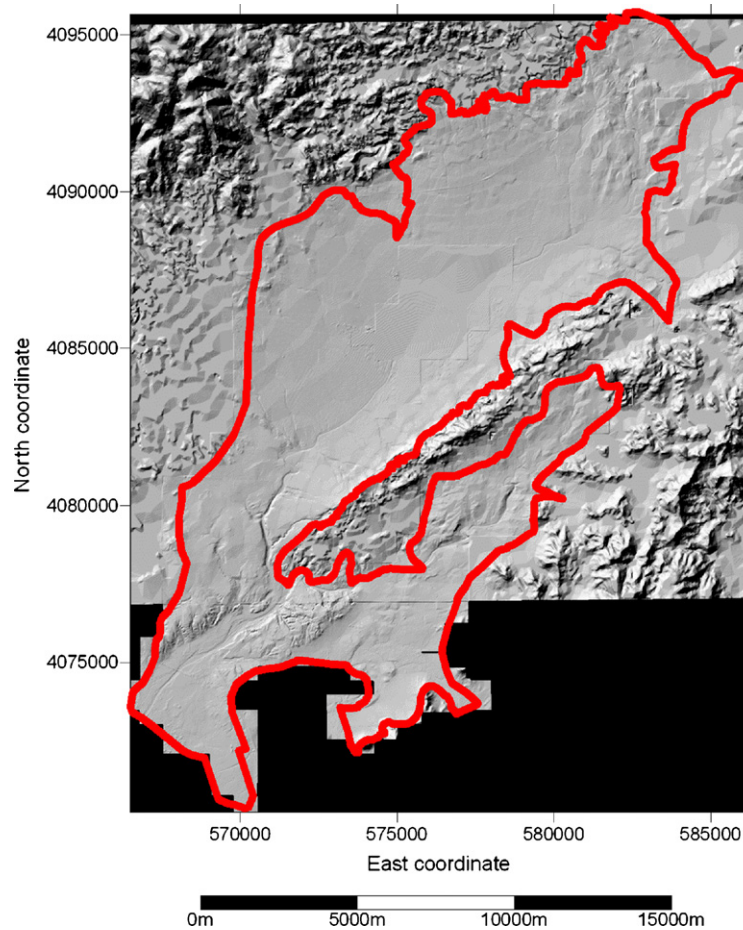


Fig. 5. Perimeter of the working area superimposed on Shaded relief of Nijar digital elevation model. Axes north and east are graduated in meters using UTM projection zone 30.

### 3.3. Digital terrain model

For the internal quality control of the DTM, a comparison was made between the DTM surface and the check points heights. It is important to indicate that it has been necessary to discard all the points that were not located on the terrain, for as we have stated previously, the DTM generated does not include the micro-relief elements. The maximum error observed, 56 cm, is attributed to the location of the original point at the top of a building. The level of comparison was calculated deducting the height of the building from the height obtained from GPS. In those areas with a high slope (e.g. steep cliff, vertical walls, etc.), the DTM may cause problems at the interpolation stage, a circumstance that would explain the error observed in this kind of points.

Anyway, DTM presented a  $2\text{ m} \times 2\text{ m}$  spacing grid format and a vertical mean root square error (RMSE) of 0.3 m. Thus, it is a high accuracy DTM suitable for cartography at 1:1000 scale and contour interval around 1 m. In Fig. 5 can be observed the perimeter of the working area superimposed on DTM shaded relief.

### 3.4. Orthoimages

These are geo-referenced orthophotographs with a very high geometric resolution of 0.10 m/pixel and a radiometric resolution of 24 bits (eight bits per RGB channel). These images, with a planimetric accuracy compatible with a 1:1000 scale, represent an extraordinary source of thematic information for the GIS.

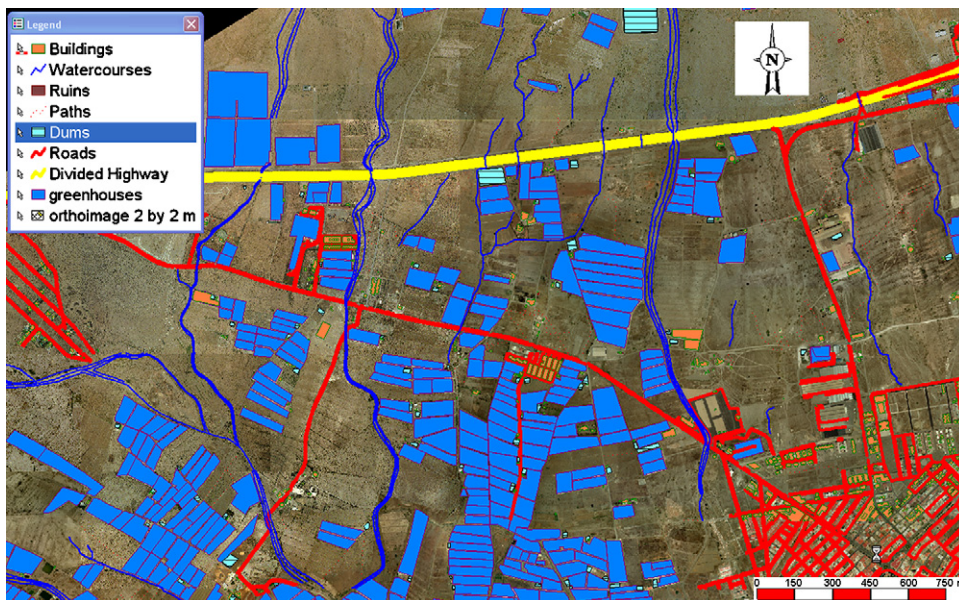


Fig. 6. Information compiled in the GIS Geomedia Professional. Map window with the features structured by layers. The orthoimage is another layer (background).

### 3.5. Integration of cartographic information on a GIS

The restitution of planimetric features from stereo models (stereocompilation) using DPWs possibilities allowed us to transfer the basic vectorial cartography to the database of the GIS Geomedia Professional 5.1. The obtained vectorial cartography in DWG format presented an accuracy which is compatible with the 1:1000 scale. It represents the geometric and topological information, i.e. constitutes the skeleton of the projected GIS. The different vectorial features obtained were classified in covers or layers (roads, paths, greenhouses, buildings, irrigation pools, etc.). Moreover, two additional covers of undoubted value were added: high resolution orthoimages and 2 m  $\times$  2 m spacing DTM.

In Fig. 6 can be observed a map window of the cartography included in Geomedia. Please note the orthoimage cover (background) on which the features are superimposed. The DTM is integrated as one more raster cover, which permits us to provide the GIS with the 3D characteristics required for some of the applications that will be demanded from it.

### 3.6. Area-based costs for making the proposed basic digital cartography

In Table 2 the area-based costs are shown for the different activities involved in the proposed basic digital cartography using photogrammetric mapping from aerial photography. The activities include aerial photography, photo control requirements and map production. For each of these activities, the cost estimates have been further stratified into categories that compose the second level of the hierarchy. For example, map production includes aerotriangulation, stereocompilation and conversion to CAD format (Lyon et al., 1995). The costs are approximately equal to those of the Spanish mapping commercial environment, including value-added tax or VAT (Spanish standard rate is 16% at present), and they have been estimated for a working area of around 20,000 ha. Obviously, the economic scale effect could diminish these costs when larger areas need to be mapped. On the other hand, 7.5% of the working area has been considered as an urban area of medium cultural density. As one can calculate from Table 2 the total cost of mapping 20,000 ha would be around 494,000 €, 16% VAT included. It could be considered as quite reasonable, above all taking into account that products obtained are fully compatible with 1:1000 scale digital cartography (vectorial and raster) and 1 m contour interval, i.e. a very high precision digital cartography.

In Table 3 the area-based costs can be observed for generating the basic digital cartography from QuickBird high-resolution satellite imagery. The general specifications are the same as those explained in Table 2. In this case, the final



Table 2

Analysis of area-based cost (Spanish value-added tax included) for the different activities involved in making the proposed high precision basic digital cartography using photogrammetric mapping from aerial photography

| Activities   | Area-based cost (€/ha) | Working area (ha) |
|--|------------------------|-------------------|
| Color photogrammetric flight at 1:5000 scale   | 2.4                    | 20000             |
| Photograms scanning: 20 $\mu$ m and 24 bits RGB  | 0.3                    | 20000             |
| Ground control for photo control requirements  | 2.2                    | 20000             |
| Digital aerotriangulation  | 0.3                    | 20000             |
| Digital terrain model generation and edition (RMSE <sub>z</sub> $\approx$ 30 cm or 1 m contour interval)                             | 3.4                    | 20000             |
| Color orthoimages 10 cm/pixel ( $\approx$ 1:1000 scale)  | 1.3                    | 20000             |
| Urban stereocompilation and field revision, including cartographic edition and conversion to CAD format compatible with 1:1000 scale | 26.2                   | 1500              |
| Rural stereocompilation and field revision, including cartographic edition and conversion to CAD format compatible with 1:1000 scale | 13.9                   | 18500             |
| Total cost   | 24.7                   | 20000             |

cost per hectare is around half of that of the method based on photogrammetric mapping. However, the products obtained present an accuracy which is around four times lower than the one required for some of the potential applications of the GIS on a local scale (see the following section). Therefore, high-resolution satellite imagery cannot be used nowadays for basic cartography at 1:1000 scale (high accuracy applications).

### 3.7. Updating of the GIS cartographic database

Using the digital image processing of QuickBird Basic Imagery (Fig. 7), we have already achieved a global orthoimage radial accuracy of around 0.7 m (Aguilar et al., 2005b). In this case, we employed the rigorous 3D physical model of Toutin et al. (2002) with a sinusoidal resampling kernel and an accurate DTM with RMSE<sub>z</sub>  $\approx$  0.3 m.

In Table 4 we can observe the area-based costs for updating the basic digital cartography produced in the last step of one QuickBird Basic Imagery scene (Bundle product: panchromatic and multispectral imagery). The costs are close to those of the Spanish mapping commercial environment, including also VAT, and have been estimated for a working area of around 20,000 ha. Furthermore, 7.5% of the working area has been considered as an urban area of medium cultural density. The costs are calculated supposing that around 5% of the basic cartography must be updated. The ground control points and DTM obtained in the generation of the basic cartography can be used in the sensor orientation, geopositioning and orthoimages generation. The final cost of 1.5 €/ha could be considered very reasonable. Note that in addition to the colour orthoimages, the near infrared band can be employed for the supervised digital image classification of greenhouses, vegetation, irrigation pools and so on.

Table 3

Analysis of area-based cost (Spanish value-added tax included) for the different activities involved in making the proposed basic digital cartography using high-resolution QuickBird imagery

| Activities   | Area-based cost (€/ha) | Working area (ha) |
|--|------------------------|-------------------|
| QuickBird Basic Stereo Pair acquisition  | 1.2                    | 20000             |
| Ground control for image control requirements  | 0.29                   | 20000             |
| Sensor orientation and geopositioning  | 0.1                    | 20000             |
| Digital terrain model generation and edition (RMSE <sub>z</sub> $\leq$ 1 m or 2–3 m contour interval)                                | 3.4                    | 20000             |
| Orthoimages 60 cm/pixel ( $\approx$ 1:5000 scale)  | 0.7                    | 20000             |
| Urban stereocompilation and field revision, including cartographic edition and conversion to CAD format compatible with 1:4000 scale | 13.1                   | 1500              |
| Rural stereocompilation and field revision, including cartographic edition and conversion to CAD format compatible with 1:4000 scale | 7                      | 18500             |
| Total cost   | 13.15                  | 20000             |

Note that in this case, and due to the limited geometric resolution of satellite imagery, the final scale of produced basic digital cartography would be around 1:4000.



Fig. 7. Detail of the full panchromatic QuickBird Basic Imagery of the region of Nijar (19th December 2004).

Classification results with texture analysis based on homogeneity are shown in Fig. 8. To evaluate the accuracy, a stratified random sampling was carried out, comprising 200 sample points, to calculate the overall accuracy (86%) and kappa coefficient (0.84). The neural network classification designed can be considered previous to the automatic detection of land use/cover changes. If an artificial neural network can differentiate classes adequately, it can be possible to detect its changes using multi-temporal data. It will require a generalization of our current artificial neural network and a different strategy for its training.

On the other hand, the treatment of QuickBird stereoscopic pairs could perform a vertical accuracy of about 46–50 cm (0.6–0.7 ground pixel size), as we can observe in a recent work published by Noguchi et al. (2004). In this work, a bias-compensated rational polynomial coefficients (RPCs) bundle adjustment is used for an accurate modelling of the sensor orientation of QuickBird imagery. The approximate area-based cost of updating the DTM using QuickBird stereoscopic pairs could be of around 4.7 €/ha (see Table 3 where we have summed the cost of stereo pair acquisition, sensor orientation and geopositioning, and DTM generation and edition). Nevertheless, nowadays QuickBird imagery with stereoscopic coverage is difficult and complex to acquire and, furthermore, there is not available record of QuickBird stereo pairs.

At this point, the introduction of new technologies as airborne laser scanner (LIDAR) to produce high-resolution DTMs could be interesting in the case of DTM updating. Major advantages of LIDAR technology in comparison with

Table 4

Analysis of area-based cost for the different activities involved in updating the proposed basic digital cartography using high-resolution satellite imagery (QuickBird)

| Activities   | Area-based cost (€/ha)                      | Working area (ha) |
|--|---|-------------------|
| One QuickBird Basic Imagery scene acquisition (bundle product: panchromatic and multispectral imagery)                               | 0.35  | 20000             |
| Ground control for image control requirements  | Done in the generation of basic cartography | 20000             |
| Sensor orientation and geopositioning  | 0.1   | 20000             |
| Digital terrain model generation and edition   | Done in the generation of basic cartography | 20000             |
| Orthoimages 60 cm/pixel ( $\approx 1:5000$ scale)  | 0.7   | 20000             |
| Urban stereocompilation and field revision, including cartographic edition and conversion to CAD format compatible with 1:4000 scale | 13.1  | 75                |
| Rural stereocompilation and field revision, including cartographic edition and conversion to CAD format compatible with 1:4000 scale | 7   | 925               |
| Total cost   | 1.5   | 20000             |



Fig. 8. Detail of classified satellite image using neural network.

digital stereo photogrammetric method, when it is applied on a bare terrain (semi-arid area for instance), are density and accuracy measurements (vertical accuracy around 15–20 cm or less), high automation and fast delivery times. But these advantages are more evident in works related to mapping of forests and vegetation areas where terrain surface cannot be recorded on a photogram. Note that some laser pulses from LIDAR (tens of thousands per second) can run through forest canopy up to reach ground and then to be reflected back to the sensor. The penetration rate depends on type of trees and vegetation. This is the so-called last return. Thus, it is quite common to create an elevation grid from both ground and top-of-canopy returns. The former is a DTM while the latter, once the DTM is subtracted, becomes the canopy height model (Wynne, 2006). Within the DTM generation from LIDAR technology, it would be useful to explore the possibility of optimising the size of the grid mesh interpolated from the very dense LIDAR point cloud in terms of a pre-established vertical accuracy (Aguilar et al., 2005a).

Regarding to operational LIDAR costs, they vary a lot depending on the firm, size of the area and point density, type of post-processing, mobilisation, platform and so forth. As a general orientation, LIDAR becomes cost-competitive with photogrammetry for generating DTMs around 1 m contour interval for project sizes over 13,000–26,000 ha. Similarly, LIDAR becomes cost-competitive with photogrammetry for DTMs 0.5 m contour interval when the project size is 3000 ha or larger (Maune et al., 2001).

Another important and newly technology to be considered in digital cartography production is mapping from airborne digital photogrammetric sensor systems. Most photogrammetric cameras being sold nowadays are digital cameras which are clearly the instrument of the future, but also of the present, with very few new film cameras now being sold (Mills and Cracknell, 2006). Note that approximately 120 large format digital photogrammetric cameras are now in operation around the world. Between the numerous advantages of this kind of sensor, we could highlight basically two of them. On the one hand, several types of products from the same flight and raw images can be obtained. These outputs include high resolution panchromatic, colour RGB and colour infrared; and lower colour resolution outputs such as colour RGB, colour infrared, four band product and near infrared. Furthermore the radiometric resolution per band uses to be around 12 bits instead of the eight bits normally obtained from film scanning technology. In this way, the final product would be very suitable for remote sensing applications such as monitoring, change detection, climatic modelling, crops detection or automatic features extraction (greenhouses, roads, irrigation pools and so on). On the second hand, imagery from digital cameras is ready for the exploitation process within the end-to-end workflow. Nor film scanning neither interior orientation is necessary because the relationship between pixel and image coordinates is



constant and is determined during the calibration procedure. Moreover, most airborne digital cameras used at present incorporate GPS and IMU (inertial measurement system) for obtaining the camera absolute position and orientation, respectively (exterior orientation for each image). This procedure, commonly called direct geopositioning, precludes the need for rigorous block aerotriangulation while meeting sub-meter accuracies. Obviously, this technology notably shortens the delivery time of the final product.

Regarding to area-based costs related to digital mapping from airborne digital photogrammetric cameras imagery, it is difficult to find out reliable prices, perhaps because the market is not too stable yet. Furthermore, we must take into account that comparison between cartographic products obtained from analog and digital airborne cameras is also very complex because outputs are usually quite different respect to their geometric and radiometric resolution, delivery time, materials and labour costs implied and so on, as we mentioned before. Note that digital photogrammetric cameras are still very expensive, and so annual depreciation cost should be included in the area-based cost study as a function of the area covered per year. Therefore, it would be more suitable to afford the aforementioned study as a part of a further work where also data fusion should be included. In fact, there is a growing tendency to obtain earth-data from more than one sensor on the same flight (data fusion). For instance, this is the case of airborne rapid imaging for emergency support (ARIES) project (Schuckman and Hoffman, 2005), in which data being acquired in the aircraft are beamed to the ground during flight for near-real-time processing, product development and dissemination. Colour optical imagery is captured using an airborne digital camera, meanwhile a LIDAR system is used to acquire laser range and timing information which later is processed into a georeferenced DTM. A GPS/IMU system allows the direct geopositioning of images and LIDAR data at the same time. The georeferenced images are orthorectified using the LIDAR-derived DTM and then automatically tiled. This is only an example of the several ways in that current earth observation technologies can give response to the necessities and demands of our society.

### 3.8. *Some practical applications of the methodology proposed*

The design of the primary and secondary irrigation network of the region has been based on the cartography generated. For the optimal location of the gravity irrigation pools that regulate the irrigation system, multicriteria and/or multiobjective decision-making methods have been utilised.

In the latter case, the centroids and the area of each greenhouse were determined in order to spatially locate the points of demand and the amount of water required ( $\text{m}^3/\text{ha}$ ). The zones where it was not advisable to locate the pools were excluded (environmentally relevant zones, villages, scarcity of free terrain, lines of communication, ravines, etc.). DTM was used to establish the areas with a sufficiently high level to supply water to all the greenhouses due to gravity.

The Geomedia Grid<sup>TM</sup> module integrated in Geomedia Professional allows raster analyses such as those known as “Corridor Analyses”. The determination of “cost distances” is understood in this case as the cost incurred by transporting water to each consumption unit (greenhouse). The term cost distances arises from the consideration that, as we move across the space we incur costs of time, money and effort, which can be anisotropic or isotropic, according to whether the direction of the movement affects or not the value of the function or friction surface of each pixel. Once the cost surfaces have been computed, geomedia grid can assess what is called the lower cost path for the transportation of water between two points (pool and greenhouse). The aim of this is simply to determine the least costly network outline for the circulation of water between the pool and the greenhouse.

A similar application would be the study of the best location for a compost plant to treat the vast amounts of organic crop residues in the region from a multicriteria perspective (capacity to house a compost plant and minimal transport costs), as described in Parra (2004).

## 4. Conclusion

From the perspective of arranging and planning the rural environment, a photo-interpretation of high resolution orthoimages and their integration in a GIS allow the devising of thematic maps of the land cover and use. The knowledge of the cover and use of the ground, and its evolution in time, represent a fundamental aid in the preparation of environmental quality indexes. In applications aimed at rural environments, these thematic maps, together with a high accuracy DTM, facilitate on the one hand a rational arrangement of the territory, whilst on the other hand they assist the preparation and tracking of agricultural environmental indicators that will allow us to value the “health” of our farming systems, a line of investigation which represents a major concern within the European Union (EEA, 2001).



## Acknowledgements

The authors are grateful to Dr. Jorge Delgado and Dr. Javier Cardenal, University of Jaén (Spain), and the Public Enterprise for Agriculture and Fishery of Andalusia (D.a.p.) for their collaboration in the preparation of this study within the project “Basic Cartography for the Campo de Níjar (Almería) Irrigation Project”. The authors would like to thank two anonymous reviewers whose comments have notably improved the manuscript.

## References

- Ackermann, F., 1996. Some Considerations About Automatic Digital Aerial Triangulation. OEEPE Official Publication No. 33, OEEPE Workshop on Application of Digital Photogrammetric Workstations, 157–164.
- Aguilar, F.J., Agüera, F., Aguilar, M.A., Carvajal, F., 2005a. Effects of terrain morphology, sampling density and interpolation methods on Grid DEM accuracy. *Photogramm. Eng. Rem. Sens.* 71 (7), 805–816.
- Aguilar, M.A., Aguilar, F.J., Sánchez, J., Carvajal, F., Agüera, F., 2005b. Geometric correction of QuickBird high resolution panchromatic images. In: *Proceedings of the XXII International Cartographic Conference (ICC2005)*, The International Cartographic Association, A Coruña, Spain (CD-ROM).
- Ararkere, S., Molnau, M., 1994. Performance of Agricultural Non-point Source Pollution in the Pacific Northwest. Paper No. 942156. American Society of Agricultural Engineers, St. Joseph, MI, USA.
- Burrough, P.A., McDonnell, R.A., 1998. *Principles of Geographical Information Systems*. Oxford University Press, Oxford.
- Davis, C.H., Wang, X., 2001. High-resolution DEMs for urban applications from NAPP photography. *Photogramm. Eng. Rem. Sens.* 67 (5), 585–592.
- DigitalGlobe Inc., 2006. QuickBird Imagery Products. Product Guide. Electronic document in pdf format. [http://www.digitalglobe.com/product/product\\_docs.shtml](http://www.digitalglobe.com/product/product_docs.shtml), last accessed December 12, 2006.
- Franklin, W.R., 2000. Applications of analytical cartography. *CaGIS J.* 27 (3), 225–237.
- EEA, 2001. Towards Agri-environmental Indicators. Integrating Statistical and Administrative Data With Land Cover Information. Reference No. 6. European Environment Agency, Copenhagen, Denmark.
- Haralick, R.M., Shanmugan, K., Dinstein, I., 1973. Textural features for image classification. *IEEE Trans. Syst. Man Cybern.* 3 (6), 610–621.
- Haralick, R.M., Sternberg, S.R., Zhuang, X., 1987. Image analysis using mathematical morphology. *IEEE Trans. Pattern Anal. Mach. Intell.* 9 (4), 532–550.
- Karras, G.E., Mavrogenneas, N., Mavrommati, D., Tsikonis, N., 1998. Tests on automatic DEM generation in a digital photogrammetric workstation. *Int. Arch. Photogramm. Rem. Sens.* 32 (2), 136–139.
- Kiema, J.B.K., 2002. Texture analysis and data fusion in the extraction of topographic objects from satellite imagery. *Int. J. Rem. Sens.* 28, 513–519.
- Lyon, J.G., Falkner, E., Bergen, W., 1995. Estimating cost for photogrammetric mapping and aerial photography. *J. Survey. Eng.* 121 (2), 63–86.
- Maune, D.F., Black, T.A., Constance, E.W., 2001. DEM user requirements. In: Maune, D.F. (Ed.), *Digital Elevation Model Technologies and Applications: The DEM Users Manual*. American Society of Photogrammetry and Remote Sensing, Bethesda, MD, pp. 441–460.
- McGlone, C., Mikhail, E., Bethel, J. (Eds.), 2004. *Manual of Photogrammetry*, 5th ed. American Society of Photogrammetry and Remote Sensing, Bethesda, MD.
- Mikhail, E., Bethel, J., McGlone, C., 2001. *Introduction to Modern Photogrammetry*. John Wiley & Sons, New York.
- Mills, J.P., Cracknell, A.P., 2006. ISPRS commission I symposium: from sensor to imagery. Conference report. *Photogramm. Rec.* 21 (116), 398–401.
- Noguchi, M., Fraser, C.S., Nakamura, T., Shimono, T., Oki, S., 2004. Accuracy assessment of Quickbird stereo imagery. *Photogramm. Rec.* 19 (106), 128–137.
- Novak, K., 1992. Rectification of digital imagery. *Photogramm. Eng. Rem. Sens.* 58 (3), 339–344.
- Pandey, V.K., Panda, S.N., Sudhakar, S., 2005. Modelling of an agricultural watershed using remote sensing and a geographic information system. *Biosystems Eng.* 90 (3), 331–347.
- Parra, S., 2004. Economic Analysis of the Valuation of Biological Agricultural Waste. Application to the evaluation of two alternative projects in the Almería's protected horticulture. Unpublished PhD diss. University of Almería, Department of Agricultural Engineering, Almería, Spain.
- PCI Geomatica, 2003. *PCI Geomatica for Windows*. Ver. 9.1.7. Ontario, Canada: PCI Geomatics Enterprises Inc.
- Richter, R., 1990. A fast atmospheric correction algorithm applied to LANDSAT TM images. *Int. J. Rem. Sens.* 11 (1), 159–166.
- Rogoswki, A.S., 1996. GIS modelling of recharge on a watershed. *J. Environ. Qual.* 25 (3), 463–474.
- Rumelhart, D.E., Durbin, R., Golden, R., Chauvin, Y., 1995. Backpropagation: the basic theory. In: Chauvin, Y., Rumelhart, D.E. (Eds.), *Backpropagation: Theory, Architectures and Applications*. Lawrence Erlbaum, Hillsdale, NJ, pp. 1–34.
- Schuckman, K., Hoffman, G.R., 2005. ARIES: technology fusion for emergency response. *Photogramm. Eng. Rem. Sens.* 71 (4), 357–360.
- TGO, 2002. *Trimble Geomatics Office for Windows*. Ver. 1.6. Dayton, OH: Trimble Navigation Ltd.
- Toutin, T., Chénier, R., Carboneau, Y., 2002. 3D models for high resolution images: examples with QuickBird, IKONOS and EROS. In: *Proceedings of the Joint International Symposium on Geospatial Theory, Processing and Applications, ISPRS*, Ottawa, Canada (CD-ROM).
- Tsoukalas, H.L., Uhring, E.R., 1997. *Fuzzy and Neural Approaches in Engineering*. John Wiley & Sons, New York.
- Wang, L., Sousa, W.P., Gong, P., Biging, S., 2004. Comparison of IKONOS and QuickBird images for mapping mangrove species on the Caribbean coast of Panama. *Rem. Sens. Environ.* 91, 432–440.

- Wei, J., Leberg, P., 2002. A GIS-based approach for assessing the regional conservation status of genetic diversity: an example from Southern Appalachians. *Environ. Manag.* 29 (4), 531–544.
- Wolf, P.R., Dewitt, B.A., 2000. *Elements of Photogrammetry with Applications in GIS*, 3rd ed. McGraw-Hill, New York.
- Wu, J., Wang, D., Bauer, M.E., 2005. Image-based atmospheric correction of QuickBird imagery of Minnesota cropland. *Rem. Sens. Environ.* 99 (3), 315–325.
- Wynne, R., 2006. Lidar remote sensing of forest resources at the scale of management. *Photogramm. Eng. Rem. Sens.* 72 (12), 1310–1314.
- Xiao, P., Zhao, X., Li, D., 2002. Land use/cover change detection on artificial neural networks and wavelet based texture analysis. *Int. Arch. Photogramm. Rem. Sens.* 34 (2), 535–540.